Alpha oscillations in the human brain implement distractor suppression independent of target selection

Malte Wöstmann, Mohsen Alavash, & Jonas Obleser
Department of Psychology, University of Lübeck, Lübeck, Germany

Corresponding authors:
Malte Wöstmann (malte.woestmann@uni-luebeck.de); Jonas Obleser (jonas.obleser@uni-luebeck.de)

Keywords: attention, selection, suppression, alpha oscillations, auditory

Abstract

In principle, selective attention is the net result of target selection and distractor suppression. The way in which both mechanisms are implemented neurally has remained contested. Neural oscillatory power in the alpha frequency band (~10 Hz) has been implicated in the selection of to-be-attended targets, but there is lack of empirical evidence for its involvement in the suppression of to-be-ignored distractors. Here, we use electroencephalography (EEG) recordings of N = 33 human participants to test the pre-registered hypothesis that alpha power directly relates to distractor suppression and thus operates independently from target selection. In an auditory spatial pitch discrimination task, we modulated the location (left vs right) of either a target or a distractor tone sequence, while fixing the other in the front. When the distractor was fixed in the front, alpha power relatively decreased contralaterally to the target and increased ipsilaterally. Most importantly, when the target was fixed in the front, alpha lateralization reversed in direction for the suppression of distractors on the left versus right. These data show that target-selection–independent alpha power is involved in distractor suppression. While both lateralized alpha responses for selection and for suppression proved reliable, they were uncorrelated and distractor-related alpha power emerged from more anterior, frontal cortical regions. Lending functional significance to suppression-related alpha oscillations, alpha lateralization at the individual, single-trial level was predictive of behavioral accuracy. These results fuel a renewed look at neurobiological accounts of selection-independent suppressive filtering in attention.

Significance statement

We tested whether the human brain implements a mechanism to suppress distraction independent of target selection. When we presented participants with targets sounds in the front, anticipated distraction on the left versus right increased the power of 10-Hz alpha oscillations in the contralateral hemisphere in the electroencephalogram. Critically, lateralized alpha responses for target selection and distractor suppression were reliable, independent of each other, and generated in more anterior, frontal regions for suppression versus selection. Prediction of single-trial task performance from alpha modulation after stimulus onset agrees with the view that alpha modulation bears direct functional relevance as a neural implementation of attention. Results demonstrate that the neurobiological foundation of attention implies a selection-independent alpha oscillatory mechanism to suppress distraction.

Introduction

Human goal-oriented behavior requires both, the selection of relevant target information and the suppression of irrelevant distraction. Although foundational theories of attention implied some form of distractor suppression [e.g., 1, 2], different neural implementations of suppression are conceivable. On the one hand, suppression might be contingent on selection, meaning that distractors outside the focus of attention are suppressed automatically [3]. On the other hand, distractor suppression might be an independent neuro-cognitive process [4] that adapts to changing characteristics of the distractor even in case the focus of attention is unchanged.

The power of brain oscillations in the alpha frequency band (~10 Hz) robustly tracks when humans shift their focus of attention between sensory modalities [5-7], to time points of anticipated target presentation [8, 9], or from one location in space to another [10, 11]. Since alpha power drops in brain regions related to processing upcoming target stimuli [7], and since lower alpha power correlates with increased neural responses to the target [12, 13] and enhanced behavioral measures of target detection [14], low alpha power is considered a signature of enhanced neural excitability to support target selection.

At the same time, alpha power does increase in brain regions that process distracting stimuli. Although high alpha power is considered a brain state of inhibited neural processing [15-17], evidenced also by negative correlation of alpha power and brain activity measured in functional magnetic resonance imaging (fMRI; [18]), it is unclear at present whether high alpha power constitutes an independent signature of distractor suppression or a by-product of target selection [19].

To study the contribution of alpha oscillations to attentional selection and suppression, neuroscientists have used spatial cueing of an upcoming target location under competing distraction at another location. Across modalities, target cueing induces alpha power lateralization, that is, alpha power decreases in the hemisphere contralateral to the target and increases in the ipsilateral hemisphere [20-22]. Alpha lateralization bears behavioral relevance: It is stronger for correct than incorrect responses to the target stimulus [20, 23]; and it modulates behavioral responses to the target if participants' endogenous alpha lateralization is stimulated transcranially (magnetically [24]; or electrically [25]).

Critically, previous studies often confounded target and distractor location by design [e.g., 23, 26, 27]: Whenever the target appeared on the left, the distractor was presented on the right, and vice versa. To unambiguously assign alpha lateralization to selection versus suppression, it is necessary to physically decouple target and distractor location during spatial attention. Addressing this, we here disentangled this conundrum by fixing the position of either an auditory target or distractor

stimulus in the front of the listener. We then only varied the respective other stimulus to come from either the left or right side.

We find that lateralized alpha power is an autonomous (i.e., target-independent) signature of suppression that can track the location of the distractor. The lateralization of alpha power proves as a reliable neural signature, separating selection from suppression within individuals and in their underlying neural generators. Finally, the instantaneous degree of alpha lateralization after, but not prior to, stimulus onset predicts trial-by-trial variations in behavioral accuracy for detecting small pitch changes in the target sound.

Results

Participants (N = 33) performed a spatial pitch-discrimination task (Fig. 1A; adopted from [28]). The loudspeaker setup changed blockwise between front-and-left or front-and-right, with one of the two loudspeakers serving as target and the other as distractor on each trial. A cue tone in the beginning of each trial indicated the location of the target loudspeaker. Participants had to report whether the ensuing tone sequence at the target location increased or decreased in pitch. A distracting tone sequence was presented simultaneously by the other loudspeaker. To avoid ceiling- and floor performance, the pitch difference within both tone sequences was titrated throughout the experiment (average pitch difference = 0.339 semitones; SD = 0.524), using an adaptive procedure to target a proportion of ~0.71 correct responses. Average proportion correct was 0.715 (between-subject SD: 0.044).

Before testing the hemispheric lateralization of oscillatory power, we inspected overall power dynamics averaged across experimental conditions (Figure 1 B&C). As commonly observed in auditory attention tasks [29-31], power in the alpha frequency band (8–12 Hz) at parietal electrodes relatively increased after trial onset and decreased in the end of a trial before participants performed a behavioral response.

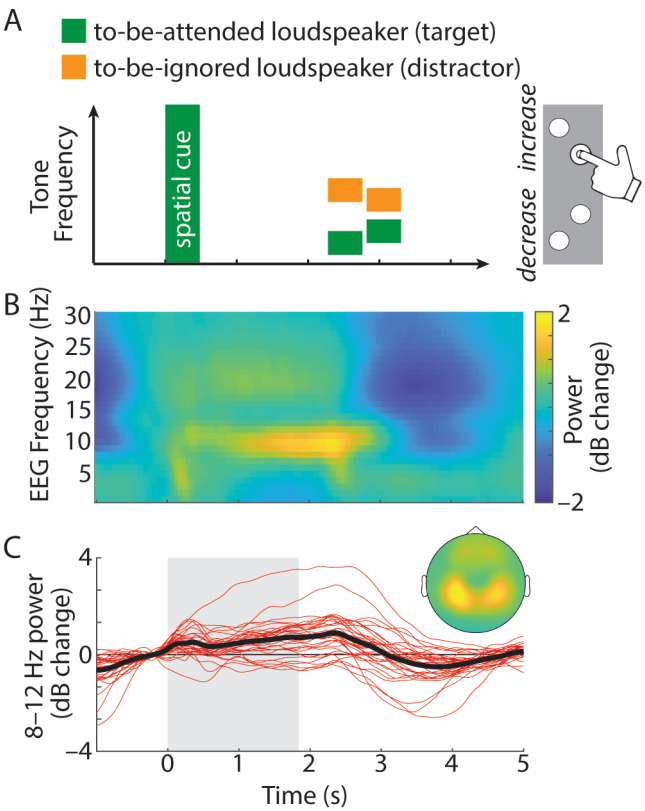

Figure 1. (**A**) Trial design. Presentation of a broad-band auditory cue (0–10.9 kHz; 0.46 s) was followed by a jittered silent interval (1.47–2.48 s). Next, two tone sequences, each consisting of two brief (0.46 s) complex tones, were presented at different locations (front, left, or right). Fundamental frequencies of low-frequency tones within each sequence were fixed at 193 and 300 Hz; frequencies of high-frequency tones were titrated throughout the experiment. Participants had to judge whether the target tone sequence at the cued location had increased or decreased in pitch. Participants also indicated confidence in their judgement (high: outer buttons; low: inner buttons). (**B**) Time-frequency representation of oscillatory power (relative to a pre-trial baseline; –0.5 to 0 s; in decibel (dB) change), averaged across N = 33 participants and all (64) scalp electrodes. (**C**) Thin red lines show single-subject alpha power (8–12 Hz) time courses; thick black line shows average; topographic map shows average 8–12 Hz power from 0 to 1.9 s (grey box).

Alpha lateralization tracks target location independent of distractor. We tested whether alpha power would track the spatial location of the to-be-selected target stimulus (left vs. right) under fixed distraction from the front. To this end, we contrasted alpha power during the anticipation of tone sequences (0–1.9 s) for trials with a target on the left versus right side (Fig. 2 A&B). Alpha power relatively increased in parietal, occipital, and inferior temporal regions in the hemisphere ipsilateral to the cued target location, and decreased contralaterally. Accordingly, the lateralization index ($LI_{selection}$), which quantifies the difference in lateralized alpha power at left-minus-right parieto-occipital electrodes, was significantly positive (CI_{95} = [0.033; 0.06]; *permutation p-value* < 0.001; see Fig. S1 for time- and frequency-resolved lateralization indices).

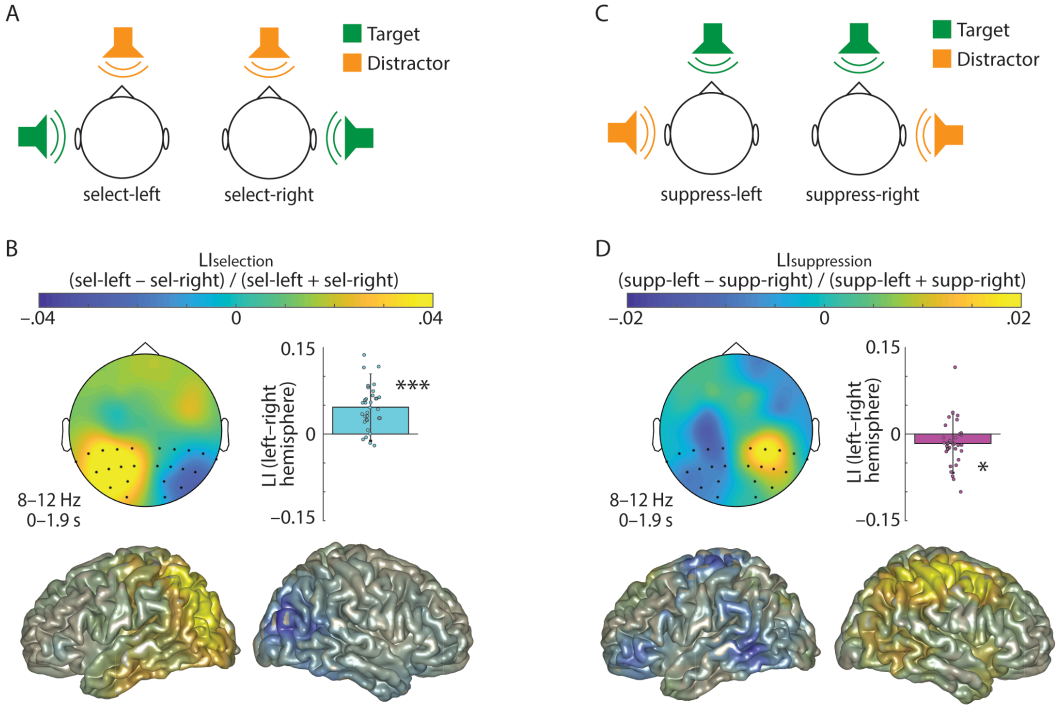

Figure 2. (**A**) Schematic illustration of task setup in select-left and select-right trials. (**B**) Topographic map and cortical surfaces show the lateralization index to contrast select-left and select-right trials under fixed distraction from the front ($LI_{selection}$). The lateralization index was calculated for 8–12 Hz alpha power during anticipation of tone sequences (0–1.9 s). Bar graph, error bar, and dots show average, ±1 between-subject SEM, and single-subject differences of LI for highlighted parieto-occipital electrodes on the left versus right hemisphere, respectively. (**C&D**) Same as A&B, but for the lateralization index for suppression of lateralized distractor stimuli ($LI_{suppression}$). * $p < 0.05$; *** $p < 0.001$.

Alpha lateralization tracks distractor location independent of target. The most important objective of the present study was to test whether lateralized alpha power contains also a neural signature of distractor suppression, independent of target selection. To test this, we contrasted alpha power for trials with the target stimulus fixed in the front but with an anticipated distractor on the left versus right side (Fig. 2 C&D). As predicted, the location of a to-be-suppressed distractor modulated alpha power orthogonally to target selection: Alpha power relatively increased in parietal, posterior temporal, and frontal lobe regions in the hemisphere contralateral to the distractor and decreased ipsilaterally. Accordingly, the lateralization index ($LI_{suppression}$) at parieto-occipital electrodes on the left versus right hemisphere was significantly negative (CI_{95} = [–0.03; –0.002]; *permutation p-value* = 0.0202; no contamination of lateralized EEG responses by saccadic eye movements, see Fig. S2).

Having established EEG signatures of target selection ($LI_{selection}$) and distractor suppression ($LI_{suppression}$), we tested reliability of these signatures. Only if they are sufficiently reliable, meaning that results on repeated tests correlate positively, any relation or difference between the two signatures can be interpreted in a meaningful way. We divided each participant's data into three consecutive

portions and found significant positive values of the reliability metric Cronbach's Alpha (CA) of alpha lateralization for target selection ($LI_{selection}$; *CA* = 0.602; *permutation p-value* = 0.001) and distractor suppression ($LI_{suppression}$; *CA* = 0.522; *permutation p-value* = 0.006).

Alpha signatures of selection and suppression operate independently. As for a potential hierarchy between alpha mechanisms of selection versus suppression, we tested whether anticipation of to-be-selected targets induces stronger alpha lateralization than anticipation of to-be-suppressed distractors. The data speak clearly in favor of this hypothesis: The hemispheric difference in alpha lateralization (LI; bar graphs in Fig. 2) was significantly more positive for $LI_{selection}$ than it was negative for $LI_{suppression}$ (CI_{95} = [0.008; 0.053]; *permutation p-value* = 0.005).

We then asked, to what extent alpha lateralization for target selection and distractor suppression would relate. If the two neural signatures instantiate the same underlying cognitive faculty, participants with stronger alpha lateralization for target selection should show stronger alpha lateralization for distractor suppression as well. This would result in more positive $LI_{selection}$ being accompanied with more negative $LI_{suppression}$ and thus in a negative correlation. To the contrary, $LI_{selection}$ and $LI_{suppression}$ were not significantly correlated (Fig. 3A; $r_{Spearman}$ = 0.153; p = 0.393; BF = 0.294; see Fig. S3 for correlation on source level). Thus, alpha lateralization for target selection and distractor suppression can be considered two largely independent neural signatures.

Next, we tested whether alpha lateralization for target selection and distractor suppression might be implemented by different neural generators. To this end, we focused on differences in spatial distribution but not strength or direction of the hemispheric difference of alpha power modulation. We z-transformed each participant's lateralization indices, followed by taking their magnitudes (referred to as $LI_{selection_norm}$ and $LI_{suppression_norm}$). Indeed, neural generators of selection and suppression differed significantly: Target selection was driven by relatively stronger alpha power modulation in parieto-occipital cortex regions, primarily in the left hemisphere (pink regions in Fig. 3B). Conversely, neural generators of distractor suppression were modulated relatively stronger in more widespread, right superior and inferior parietal, inferior temporal, superior frontal, and middle frontal cortex regions (blue regions in Fig. 3B).

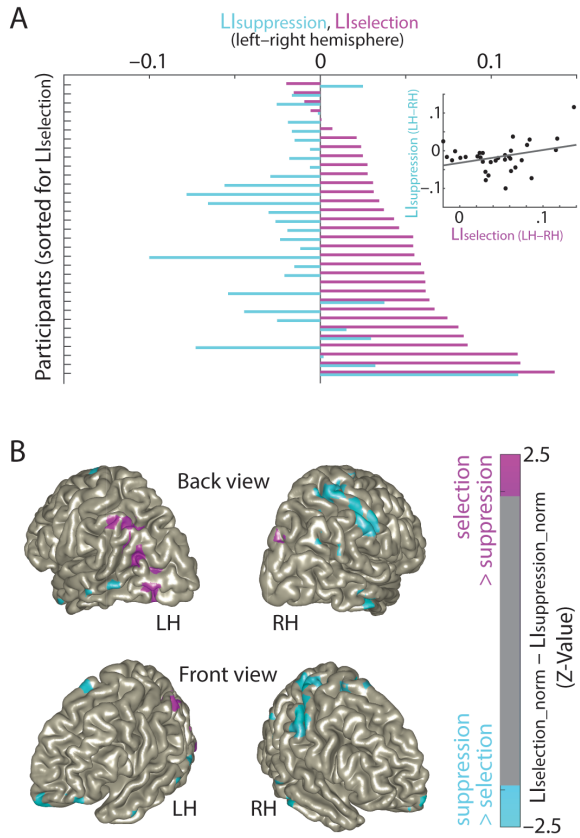

Figure 3. (**A**) Bars show single-subject alpha lateralization indices at left minus right parieto-occipital electrodes (pink: $LI_{selection}$; blue: $LI_{suppression}$), sorted for $LI_{selection}$. Inset shows scatterplot for $LI_{selection}$ and $LI_{suppression}$, with least-squares regression line (*Spearman rho* = 0.153; $p = 0.393$). (**B**) Normalization of lateralization indices on the source-level was accomplished by z-transformation of single-subject lateralization indices, followed by taking the magnitude. Brain surfaces show Z-statistics derived from dependent-samples *t*-tests for the contrast of normalized lateralization indices: $LI_{selection_norm}$ versus $LI_{supression_norm}$. Z-statistics on brain surfaces are masked in case $|Z| < 1.96$, corresponding to $p > 0.05$ for two-sided testing (uncorrected). Top: back view; bottom: front view. LH: left hemisphere; RH: right hemisphere.

Functional relation of alpha lateralization to single-trial task performance. We modeled single-trial confidence-weighted accuracy (see SI for analysis of raw accuracy and response time) on the predictors *titrated pitch difference* (within both tone sequences), *congruency of pitch direction across target and distractor tone sequence* (congruent versus incongruent), *location of lateralized loudspeaker* (left versus right), and *role of lateralized loudspeaker* (target versus distractor).

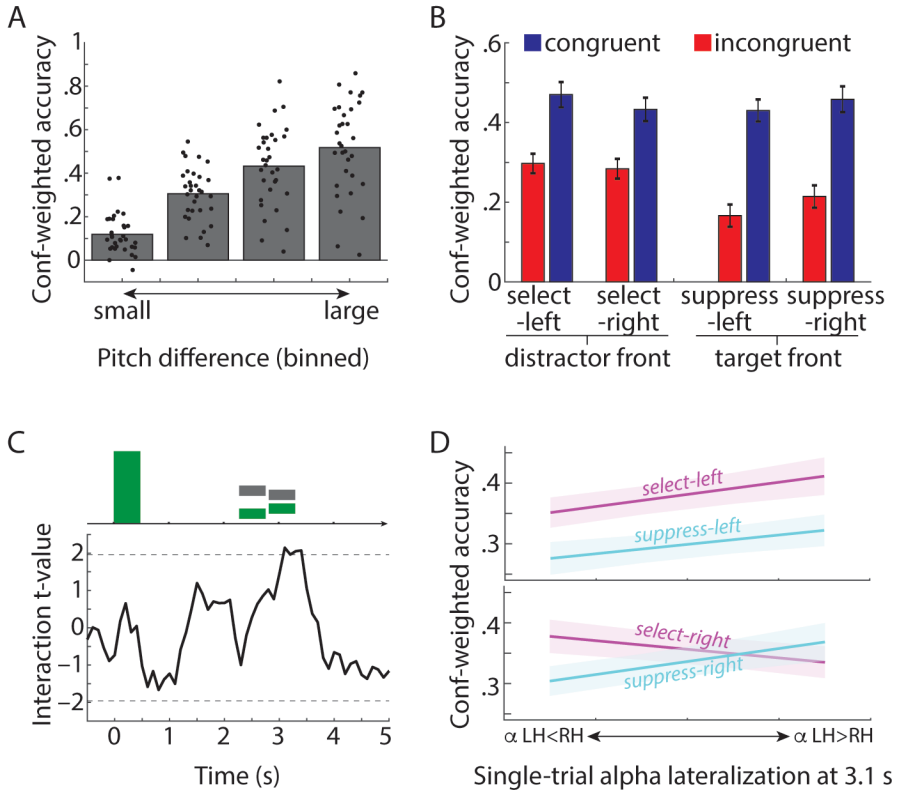

Figure 4. (**A**) Bars show average confidence-weighted accuracy as a function of the pitch difference between the two tones within each tone sequence (divided into four bins for each participant for visualization), which was titrated over the course of the experiment. Dots show single-subject data. (**B**) Bars and error bars show average ±1 between-subject SEM of confidence-weighted accuracy, separately for congruent trials (both tone sequences increasing/decreasing in pitch; blue) and incongruent trials (one tone sequences increasing and other decreasing in pitch; red). (**C**) Black solid line shows trace of t-values for the location × role of lateralized loudspeaker × single-trial alpha lateralization interaction obtained from multiple linear mixed models. Dashed lines indicate significance thresholds (*alpha* = 0.05; uncorrected). (**D**) Visualization of significant location × role of lateralized loudspeaker × alpha lateralization interaction at a latency of 3.1 s. For each participant and experimental condition, single-trial alpha lateralization values ($LI_{single\text{-}trial}$; quantifying left-versus-right hemispheric alpha power) were separated into four bins, followed by fitting a linear slope to average confidence-weighted accuracy as a function of increasing bin number. Lines show average across single-subject linear fits, shaded areas show ±1 between-subject SEM. LH: left hemisphere; RH: right hemisphere.

Confidence-weighted accuracy increased if the pitch difference between the tones within each sequence (target and distractor) was larger (Fig. 4A; $t_{16949} = 10.031$; $p < 0.001$), if tone sequences were congruent in pitch direction (Fig. 4B $t_{16949} = 8.572$; $p < 0.001$), and if the target loudspeaker was on the side compared to front (main effect role of lateralized loudspeaker: $t_{16949} = -5.622$; $p < 0.001$), which agrees with a previous study that used a similar task design [28]. The latter effect was driven by incongruent trials, evidenced by the congruency × role of lateralized loudspeaker interaction ($t_{16949} = 2.764$; $p = 0.006$). The location × role of lateralized loudspeaker interaction approached statistical significance ($t_{16949} = 1.803$; $p = 0.071$), which speaks to a tendency of higher confidence-

weighted accuracy for target selection on the left versus right but for distractor suppression on the right versus left (see SI for complete summary tables of mixed model analyses).

To test our hypothesis that lateralized alpha power predicts task performance, we added single-trial alpha lateralization ($LI_{single\text{-}trial}$) before the onset of tone sequences (0–1.9 s) to the set of predictors. Relatively higher left-than-right hemispheric alpha power should be beneficial in select-left and suppress-right trials but detrimental in select-right and suppress-left trials, reflected in a location × role of lateralized loudspeaker × alpha lateralization interaction. Against what we had hypothesized, this interaction was clearly non-significant ($t_{16941} = 0.002$; $p = 0.999$). However, when we used single-trial alpha lateralization for successive time intervals throughout a trial as predictors (in separate mixed-effects models) in an exploratory follow-up analysis, we found a weak but significant location × role of lateralized loudspeaker × alpha lateralization interaction only in a late time window in the end of tone sequence presentation (3.1–3.4 s; Fig. 4C). The interaction was driven by trials with the lateralized loudspeaker on the right side (Fig. 4D): In line with the proposed inhibitory role of alpha power, relatively higher left-hemispheric alpha power improved suppression of distractors on the right but impaired selection of targets on the right.

Discussion

The present study tested whether the human brain implements a mechanism of distractor suppression that is independent of target selection. Results show that this is the case. Under fixed presentation of auditory targets in the front, anticipation of to-be-suppressed distractors on the left versus right side induced contralateral increase and ipsilateral decrease of alpha power. Alpha lateralization for target selection and distractor suppression were not only opposite in direction but we demonstrate here that the two are reliable and independent neural signatures generated in partly distinct underlying neural networks. Exploratory analysis of the relation between alpha lateralization and behavioral task performance supports the view that alpha power modulation following stimulus onset controls the read-out of sensory objects that compete for attention.

Alpha lateralization is an autonomous signature of distractor suppression. The most important result of the present study was significant lateralization of alpha power in anticipation of distractors on the left versus right side in case the focus of attention was fixed to the front (Fig. 2C&D). This finding confirms our pre-registered hypothesis of alpha lateralization as a neural signature of target-independent (i.e., autonomous) distractor suppression (https://osf.io/bv7zs).

While neuroscience has previously shown that alpha oscillations represent an inhibitory signal that correlates with suppressed neural firing [32, 33], we demonstrate here that alpha power constitutes inhibition also in a psychological sense [4]: It signifies a participant's intention to ignore distracting sensory information. Our results clearly challenge the view that alpha oscillations are not involved in distractor suppression [19] and instead show that lateralized alpha power adapts to the location of anticipated distraction independent of selecting a target at a fixed location.

Participants in the present study made use of alpha power lateralization, although in opposite direction, to implement target selection versus distractor suppression. In this sense, alpha power is a neural signal that implements the psychological construct of an attentional filter [23, 34] to coordinate the interplay of selection and suppression. Since alpha responses for selection and suppression were reliable and uncorrelated, we consider these neural responses traits that allow to place a participant's instantiation of the attentional filter in a two-dimensional space defined by neural target selection and distractor suppression (Fig. 4).

In theory, separation of competing target and distractor can be achieved by target enhancement or by distractor inhibition. So why should the human brain implement both of these mechanisms if one would suffice? For any biological system, the magnitude of response has a limited dynamic range. Attentional selection can only enhance neural processing of the target to a finite extent. Thus, a dual mechanism that additionally implements distractor suppression is able to effectively double the separation of target and distractor [35].

Neural implementation of target selection and distractor suppression. In line with the prevalent model of alpha power as a signature of neural inhibition [15-17], relatively high alpha power in the hemisphere contralateral to a distractor indicates suppression, while low alpha power contralateral to a target indicates selection. Previous studies, which tied spatial locations of target and distractor by presenting either one left and the other right, likely observed a superposition of two underlying lateralized alpha responses that we separated in the present study.

Evidence for the involvement of alpha oscillations in neural processing of distraction comes also from studies that found alpha power modulation associated with changing features of the distractor, such as its acoustic quality [36], visual similarity to the target [37], the number of distractors [38], or continuous luminance changes in the distractor [39]. The design of the present study allowed us to trace and contrast the neural sources of lateralized alpha responses for target selection and distractor suppression, which were prominent in superior and inferior parietal cortex region that are part of the dorsal attention network [40] and involved in coding spatial locations of stimuli in the environment [41]. The apparent absence of alpha lateralization in auditory cortex regions is not unusual for auditory spatial attention tasks in the EEG [42], but auditory sources of lateralized alpha

power have been observed in the Magnetoencephalogram (MEG) during the presentation of target versus distractor speech [23].

Compared to target selection, distractor suppression induced relatively stronger alpha modulation in distributed regions including parietal, and (pre-) frontal cortex (Fig. 4). Such a pattern of frontal and parietal activations, termed multiple-demand (MD) system, has been found involved in a multitude of cognitively challenging tasks [43]. In particular, prefrontal cortex is a source of executive control [44, 45], which is crucial for the orchestration of different neural processes to implement attention. Prefrontal cortex involvement in distractor suppression has also been evidenced by its relation to performance in tasks requiring cognitive control, such as the Stroop task [e.g., 46]. Our results thus help integrate the lateralized neural alpha response to distraction into models of prefrontal cortex involvement in inhibitory cognitive control.

It is of note that direct comparison of target selection and distractor suppression is somewhat limited in the present study. A bottom-up auditory cue drew attention to the target, whereas participants had to infer that the distractor would occur at the non-cued location. Furthermore, it might in theory be possible that lateralized alpha oscillations code the relative position of the target with respect to the distractor, which was the same (i.e. 90° to the left) in select-left and suppress-right trials. However, our results clearly speak against this, since alpha lateralization for target selection and distractor suppression were not only different in strength and source origin, but were also uncorrelated.

Behavioral relevance of the lateralized alpha response. To our surprise, we did not find the hypothesized relation of single-trial alpha lateralization prior to stimulus presentation and task performance [for a study that recently reported such a relation in a different task setting, see 47]. Instead, alpha lateralization after the onset of competing tone sequences predicted single-trial pitch discrimination performance, although the relation was relatively weak. There is an ongoing debate whether alpha lateralization is a purely proactive mechanism of attentional control to prepare for upcoming target and distractor, or whether alpha lateralization also has the potency to reactively select the target and to suppresses the distractor after these have been encoded [for review of proactive and reactive mechanisms, see 48].

Our results differentiate proactive and reactive accounts of attention: While observed alpha power lateralization prior to competing tone sequences speaks to alpha lateralization as a signature of proactive attentional control, prediction of pitch discrimination performance only by post-stimulus alpha lateralization signifies the behavioral relevance of reactive attentional control [23].

Materials and Methods

Pre-registration. Prior to data recording, we pre-registered the study design, data sampling plan, hypotheses, and analyses procedures online with the Open Science Framework (OSF; https://osf.io/bv7zs).

Participants. We analyzed data of N = 33 right-handed participants (M_{age} = 23.3 years; SD_{age} = 3.9 years; 22 females). Data of three additional participants were recorded but excluded, as two of them had excessive EEG artifacts and one was unable to perform the task. Participants were financially compensated or received course credit. All procedures were approved by the local ethics committee of the University of Lübeck.

Auditory stimuli and task setup. Task design and stimuli were adapted from Dai, Best, and Shinn-Cunningham [28]. Due to a change in the stimulus sampling frequency, however, duration and pitch of auditory stimuli deviated slightly in the present study. The experiment was implemented in the Psychtoolbox [49] for Matlab, and conducted in a soundproof cabin. All auditory stimuli were presented at a sampling frequency of 48 kHz and were presented at a comfortable level of ~65 dBA.

On each trial, two tone sequences were presented concurrently at different spatial locations (front, left, or right). Each sequence consisted of two 0.46-s complex tones (fixed ISI of 46 ms), one low-pitch tone and one high-pitch tone. The pitch of the low-pitch tone was fixed at 192.7 Hz (including 32 harmonics) for one sequence and at 300.4 Hz (including 2 harmonics) for the other sequence. Throughout the experiment, the fundamental frequency of the high-pitch tone in each sequence varied in semitones relative to the low-pitch tone using an adaptive tracking procedure (two-up-one-down) to arrive at ~71 % task accuracy [50].

Tone sequences were presented in free field using a pair of loudspeakers (Logitech, x140). The location of a speaker could be either front or side (i.e., 0 or ±90 degrees azimuth relative to ear-nose-ear line). Loudspeakers were positioned at approximately 70 cm distance to the participant's head. As the main experimental manipulation, the location of the side speaker changed between left and right across blocks of the experiment. The other speaker was positioned in front of the participant throughout. There were three blocks of the experiment with the side speaker positioned on the left side, and three blocks with the side speaker on the right. The order of blocks was counter-balanced across participants, and alternated between left and right. Within each block a participant completed 96 trials (each loudspeaker served as the target in 48 trials).

Procedure. At the start of each trial, after a jittered period of ~1 sec (0.8–1.2 s), an auditory spatial cue was presented on one loudspeaker (10.9-kHz low-pass filtered Gaussian noise; 0.46 s) to inform

the participant about the target loudspeaker location. After a jittered period of ~1.8 s (right-skewed distribution; median: 1.84 s; truncated at 1.47 and 2.48 s) relative to cue offset, two tone sequences were presented concurrently. Participants reported whether the tone sequence at the target location increased or decreased in pitch and how confident they were in this response using a response box with four buttons (see Fig. 1A). Participants were instructed to fixate a cross in the middle of the response box throughout the experiment. Prior to the main experiment, a short training ensured that participants could perform the pitch discrimination task.

EEG recording and preprocessing. The EEG was recorded at 64 active scalp electrodes (Ag/Ag-Cl; ActiChamp, Brain Products, München, Germany) at a sampling rate of 1000 Hz, with a DC–280 Hz bandwidth, against a left mastoid reference (channel TP9). All electrode impedances were kept below ~30 kOhm. To ensure equivalent placement of the EEG cap, the vertex electrode (Cz) was placed at 50% of the distance between inion and nasion and between left and right ear lobes.

For EEG data analysis, we used the FieldTrip toolbox [51] for Matlab (R2013b/R2018a) and custom scripts. Offline, the continuous EEG data were filtered (1-Hz high-pass; 100-Hz low-pass) and segmented into epochs relative to the onset of the spatial cue (–2 to +6 s). An independent component analysis (ICA) was used to detect and reject components corresponding to eye blinks, saccadic eye movements, muscle activity, and heartbeat. On average 38.48 % (SD: 10 %) of components were rejected. After visual inspection of EEG time-domain data, noisy electrodes (one electrode of two participants) were interpolated using the nearest neighbor approach implemented in FieldTrip. Finally, trials in which an individual EEG channel exceeded a range of 200 microvolts were rejected. On average 568 trials (SD: 11 trials) of executed 576 trials per participant were used for further analyses.

Analysis of neural oscillatory activity. EEG data were re-referenced to the average of all electrodes and down-sampled to 250 Hz. Single-trial time-frequency representations were derived using complex Fourier coefficients for a moving time window (fixed length of 0.5 s; Hanning taper; moving in steps of 0.04 s) for frequencies 1–30 Hz with a resolution of 1 Hz.

To quantify the impact of selection and suppression, single-trial power representations (squared magnitude of complex Fourier coefficients) were calculated for individual experimental conditions: select-left, select-right, suppress-left, and suppress-right. For each participant, two lateralization indices (LI) were calculated on absolute oscillatory power (Pow). The first index quantifies oscillatory signatures of target selection:

(1) $LI_{selection} = (Pow_{select\text{-}left} - Pow_{select\text{-}right}) / (Pow_{select\text{-}left} + Pow_{select\text{-}right})$

Importantly, the second index quantifies oscillatory signatures of distractor suppression, which goes beyond what previous studies have analyzed:

$$(2)\quad LI_{suppression} = (Pow_{suppress\text{-}left} - Pow_{suppress\text{-}right}) / (Pow_{suppress\text{-}left} + Pow_{suppress\text{-}right})$$

For statistical analyses, we followed our pre-registered analysis plan (https://osf.io/bv7zs). In brief, we averaged each lateralization index (LI) across frequencies in the alpha band (8–12 Hz), the time interval from cue onset to earliest tone sequence onset (0–1.9 s), separately for two sets of 12 left- and 12 right hemispheric occipito-parietal electrodes (TP9/10, TP7/8, CP5/6, CP3/4, CP1/2, P7/8, P5/6, P3/4, P1/2, PO7/8, PO3/4, and O1/2). For statistical comparisons of the LI (left vs. right hemisphere; selection vs. suppression), we used non-parametric permutation tests. The reported *p*-value corresponds to the relative number of absolute values of 10,000 dependent-samples *t*-statistics computed on data with permuted condition labels exceeding the absolute empirical *t*-value for the original data.

To determine reliability of lateralization indices, we divided each participant's trials into three consecutive portions (each consisting of approximately 192 trials, with 48 trials for each condition), followed by calculation of lateralization indices for each portion. Next, we calculated the reliability metric Cronbach's Alpha (CA) for each lateralization index across the three portions. The *p*-value for CA was derived by the relative number of permuted CAs, derived from 10,000 permutations of single-subject lateralization indices within each one of the three portions, exceeding the empirical CA [52].

For the non-significant Spearman correlation of the two lateralization indices ($LI_{selection}$, $LI_{suppression}$) we report the Bayes Factor (computed for Kendall's tau in the software Jamovi). The Bayes Factor (*BF*) indicates how many times more likely the observed data are under the alternative (H_1) compared to the null hypothesis (H_0). By convention, a $BF > 3$ begins to lend support to H_1, whereas a $BF < 0.33$ begins to lend support to H_0 [53].

EEG source analysis. We used the Dynamic Imaging of Coherent Sources (DICS) beamformer approach [54] implemented in FieldTrip. A standard head model (Boundary Element Method, BEM; 3-shell) was used to calculate leadfields for a grid of 1 cm resolution. Spatial filters were calculated from the leadfield and the cross-spectral density of Fourier transforms centered at 10 Hz with ± 2 Hz spectral smoothing in the time interval 0–1.9 s relative to cue onset. For each participant, two spatial filters were calculated to source-localize $LI_{selection}$ and $LI_{suppression}$, based on all trials with the target or distractor on the side, respectively. The spatial filter for $LI_{selection}$ was used to localize alpha power separately for select-left and select-right trials, followed by calculation of the lateralization index

$LI_{selection}$ on the source level (and accordingly for $LI_{suppression}$). Finally, source-level LIs were averaged across participants and mapped onto a standard brain surface.

Behavioral data analysis. Single-trial EEG and behavioral data were matched. Due to few missing EEG triggers, one participant's data were excluded from behavioral analyses. For remaining N = 32 participants, an average of 523 trials was used. Behavioral data were analyzed using mixed-effects models implemented in the *fitlme* function for Matlab. The response variable of interest was single-trial confidence-weighted accuracy, derived by transformation of binary accuracy into 1 and 1/3 for correct responses with respective high and low confidence, and into −1 and −1/3 for incorrect responses with respective high and low confidence [29]. As predictors, we used the titrated pitch difference (within both tone sequences), congruency of pitch direction across the two tone sequences (congruent versus incongruent), location of lateralized loudspeaker (left versus right), and role of lateralized loudspeaker (target versus distractor), with participant as a random intercept term, resulting in the linear-model expression: Confidence-weighted accuracy ~ 1 + Titrated pitch difference + Congruency of pitch direction × Location of lateralized loudspeaker × Role of lateralized loudspeaker + (1|Participant ID)

To model the relation of alpha lateralization and confidence-weighted accuracy, we included single-trial alpha lateralization ($LI_{single\text{-}trial}$) before tone sequence onset (0–1.9 s) and for a 1-s time window moving in 0.1-s steps through a trial as predictors in separate linear mixed-effects models. Single trial alpha power lateralization was quantified as the contrast of alpha power (obtained via Fourier transform using multi-tapering at 10 Hz with 2-Hz spectral smoothing) at 12 parieto-occipital left-minus-right hemispheric electrodes:

$$(3)\quad LI_{single\text{-}trial} = (POW_{left\text{-}electrodes} - POW_{right\text{-}electrodes}) / (POW_{left\text{-}electrodes} + POW_{right\text{-}electrodes}).$$

454 **References**

455 1. Broadbent, D., *Perception and Communication*. 1958, London: Pergamon.

456 2. Treisman, A.M., *Monitoring and Storage of Irrelevant Messages in Selective Attention.* Journal of
457 Verbal Learning and Verbal Behavior, 1964. **3**(6): p. 449-459.

458 3. Noonan, M.P., et al., *Selective inhibition of distracting input.* Behav Brain Res, 2018. **355**: p. 36-
459 47.

460 4. Aron, A.R., *The neural basis of inhibition in cognitive control.* Neuroscientist, 2007. **13**(3): p. 214-
461 28.

462 5. Fu, K.M., et al., *Attention-dependent suppression of distracter visual input can be cross-modally*
463 *cued as indexed by anticipatory parieto-occipital alpha-band oscillations.* Brain Res Cogn Brain
464 Res, 2001. **12**(1): p. 145-52.

465 6. Adrian, E.D., *Brain Rhythms.* Nature, 1944. **153**: p. 360-362.

466 7. de Pesters, A., et al., *Alpha power indexes task-related networks on large and small scales: A*
467 *multimodal ECoG study in humans and a non-human primate.* Neuroimage, 2016. **134**: p. 122-
468 31.

469 8. Payne, L., S. Guillory, and R. Sekuler, *Attention-modulated alpha-band oscillations protect*
470 *against intrusion of irrelevant information.* J Cogn Neurosci, 2013. **25**(9): p. 1463-76.

471 9. Rohenkohl, G. and A.C. Nobre, *alpha oscillations related to anticipatory attention follow*
472 *temporal expectations.* J Neurosci, 2011. **31**(40): p. 14076-84.

473 10. Sauseng, P., et al., *A shift of visual spatial attention is selectively associated with human EEG*
474 *alpha activity.* Eur J Neurosci, 2005. **22**(11): p. 2917-26.

475 11. Worden, M.S., et al., *Anticipatory biasing of visuospatial attention indexed by retinotopically*
476 *specific alpha-band electroencephalography increases over occipital cortex.* J Neurosci, 2000.
477 **20**(6): p. 1-6.

478 12. Gould, I.C., M.F. Rushworth, and A.C. Nobre, *Indexing the graded allocation of visuospatial*
479 *attention using anticipatory alpha oscillations.* J Neurophysiol, 2011. **105**(3): p. 1318-26.

480 13. Wöstmann, M., L. Waschke, and J. Obleser, *Prestimulus neural alpha power predicts confidence*
481 *in discriminating identical auditory stimuli.* Eur J Neurosci, 2019. **49**(1): p. 94-105.

482 14. Thut, G., et al., *Alpha-band electroencephalographic activity over occipital cortex indexes*
483 *visuospatial attention bias and predicts visual target detection.* J Neurosci, 2006. **26**(37): p.
484 9494-502.

485 15. Strauß, A., M. Wöstmann, and J. Obleser, *Cortical alpha oscillations as a tool for auditory*
486 *selective inhibition.* Frontiers in Human Neuroscience, 2014. **8:350**.

487 16. Jensen, O. and A. Mazaheri, *Shaping functional architecture by oscillatory alpha activity: gating*
488 *by inhibition.* Front Hum Neurosci, 2010. **4**: p. 186.

17. Foxe, J.J. and A.C. Snyder, *The Role of Alpha-Band Brain Oscillations as a Sensory Suppression Mechanism during Selective Attention.* Front Psychol, 2011. **2**: p. 154.
18. Laufs, H., et al., *EEG-correlated fMRI of human alpha activity.* Neuroimage, 2003. **19**(4): p. 1463-76.
19. Foster, J.J. and E. Awh, *The role of alpha oscillations in spatial attention: limited evidence for a suppression account.* Curr Opin Psychol, 2018. **29**: p. 34-40.
20. Haegens, S., B.F. Handel, and O. Jensen, *Top-down controlled alpha band activity in somatosensory areas determines behavioral performance in a discrimination task.* J Neurosci, 2011. **31**(14): p. 5197-204.
21. Bauer, M., S. Kennett, and J. Driver, *Attentional selection of location and modality in vision and touch modulates low-frequency activity in associated sensory cortices.* J Neurophysiol, 2012. **107**(9): p. 2342-51.
22. Ahveninen, J., et al., *Dynamic oscillatory processes governing cued orienting and allocation of auditory attention.* J Cogn Neurosci, 2013. **25**(11): p. 1926-43.
23. Wöstmann, M., et al., *Spatiotemporal dynamics of auditory attention synchronize with speech.* Proc Natl Acad Sci U S A, 2016. **113**(14): p. 3873-3878.
24. Romei, V., J. Gross, and G. Thut, *On the role of prestimulus alpha rhythms over occipito-parietal areas in visual input regulation: correlation or causation?* J Neurosci, 2010. **30**(25): p. 8692-7.
25. Wöstmann, M., et al., *Opposite effects of lateralised transcranial alpha versus gamma stimulation on auditory spatial attention.* Brain Stimul, 2018.
26. van Diepen, R.M., et al., *The Role of Alpha Activity in Spatial and Feature-Based Attention.* eNeuro, 2016. **3**(5).
27. Kelly, S.P., et al., *Increases in alpha oscillatory power reflect an active retinotopic mechanism for distracter suppression during sustained visuospatial attention.* J Neurophysiol, 2006. **95**(6): p. 3844-51.
28. Dai, L., V. Best, and B.G. Shinn-Cunningham, *Sensorineural hearing loss degrades behavioral and physiological measures of human spatial selective auditory attention.* Proc Natl Acad Sci U S A, 2018. **115**(14): p. E3286-E3295.
29. Wöstmann, M., et al., *Neural alpha dynamics in younger and older listeners reflect acoustic challenges and predictive benefits.* J Neurosci, 2015. **35**(4): p. 1458-67.
30. Henry, M.J., et al., *Aging affects the balance of neural entrainment and top-down neural modulation in the listening brain.* Nat Commun, 2017. **8**: p. 15801.
31. Wöstmann, M., L. Fiedler, and J. Obleser, *Tracking the signal, cracking the code: Speech and speech comprehension in non-invasive human electrophysiology.* Language, Cognition and Neuroscience, 2017. **32**(7).

32. Jensen, O., M. Bonnefond, and R. VanRullen, *An oscillatory mechanism for prioritizing salient unattended stimuli.* Trends Cogn Sci, 2012. **16**(4): p. 200-6.
33. Haegens, S., et al., *alpha-Oscillations in the monkey sensorimotor network influence discrimination performance by rhythmical inhibition of neuronal spiking.* Proc Natl Acad Sci U S A, 2011. **108**(48): p. 19377-82.
34. Lakatos, P., et al., *The spectrotemporal filter mechanism of auditory selective attention.* Neuron, 2013. **77**(4): p. 750-61.
35. Houghton, G. and S.P. Tipper, *A model of inhibitory mechanisms in selective attention*, in *Inhibitory Processes of Attention, Memory and Language*, D. Dagenbach and T. Carr, Editors. 1984, Academic Press Ltd: Florida.
36. Wöstmann, M., S.J. Lim, and J. Obleser, *The Human Neural Alpha Response to Speech is a Proxy of Attentional Control.* Cereb Cortex, 2017. **27**(6): p. 3307-3317.
37. Bonnefond, M. and O. Jensen, *Alpha oscillations serve to protect working memory maintenance against anticipated distracters.* Curr Biol, 2012. **22**(20): p. 1969-74.
38. Sauseng, P., et al., *Brain oscillatory substrates of visual short-term memory capacity.* Curr Biol, 2009. **19**(21): p. 1846-52.
39. Jia, J., F. Fang, and H. Luo, *Selective spatial attention involves two alpha-band components associated with distinct spatiotemporal and functional characteristics.* Neuroimage, 2019.
40. Sadaghiani, S., et al., *Intrinsic connectivity networks, alpha oscillations, and tonic alertness: a simultaneous electroencephalography/functional magnetic resonance imaging study.* J Neurosci, 2010. **30**(30): p. 10243-50.
41. Colby, C.L. and M.E. Goldberg, *Space and attention in parietal cortex.* Annu Rev Neurosci, 1999. **22**: p. 319-49.
42. Tune, S., M. Wöstmann, and J. Obleser, *Probing the limits of alpha power lateralization as a neural marker of selective attention in middle-aged and older listeners.* European Journal of Neuroscience, 2018.
43. Duncan, J., *The multiple-demand (MD) system of the primate brain: mental programs for intelligent behaviour.* Trends Cogn Sci, 2010. **14**(4): p. 172-9.
44. Miller, E.K. and J.D. Cohen, *An integrative theory of prefrontal cortex function.* Annu Rev Neurosci, 2001. **24**: p. 167-202.
45. Sadaghiani, S. and A. Kleinschmidt, *Brain Networks and alpha-Oscillations: Structural and Functional Foundations of Cognitive Control.* Trends Cogn Sci, 2016. **20**(11): p. 805-817.
46. Vendrell, P., et al., *The role of prefrontal regions in the Stroop task.* Neuropsychologia, 1995. **33**(3): p. 341-52.

47. Dahl, M.J., et al., *Diminished pre-stimulus alpha-lateralization suggests compromised self-initiated attentional control of auditory processing in old age.* Neuroimage, 2019. **197**: p. 414-424.
48. Geng, J.J., *Attentional Mechanisms of Distractor Suppression.* Current Directions in Psychological Science, 2014. **23**(2).
49. Brainard, D.H., *The Psychophysics Toolbox.* Spat Vis, 1997. **10**(4): p. 433-6.
50. Levitt, H., *Transformed up-down methods in psychoacoustics.* J Acoust Soc Am, 1971. **49**(2): p. Suppl 2:467+.
51. Oostenveld, R., et al., *FieldTrip: Open source software for advanced analysis of MEG, EEG, and invasive electrophysiological data.* Comput Intell Neurosci, 2011. **2011**: p. 156869.
52. Prelog, A.J., K.J. Berry, and P.W. Mielke, Jr., *Resampling permutation probability values for Cronbach's alpha.* Percept Mot Skills, 2009. **108**(2): p. 431-8.
53. Dienes, Z., *Using Bayes to get the most out of non-significant results.* Front Psychol, 2014. **5**: p. 781.
54. Gross, J., et al., *Dynamic imaging of coherent sources: Studying neural interactions in the human brain.* Proc Natl Acad Sci U S A, 2001. **98**(2): p. 694-9.

Supporting Information

Time- and frequency-resolved lateralization indices. Figure S1 shows lateralization indices ($LI_{selection}$ and $LI_{suppression}$) for frequencies 1–30 Hz and the entire time interval of an experimental trial (–1 to 5 s relative to cue onset). Lateralization of oscillatory power in the alpha frequency band (8–12 Hz) was particularly prominent after presentation of the spatial cue and decreased later during a trial.

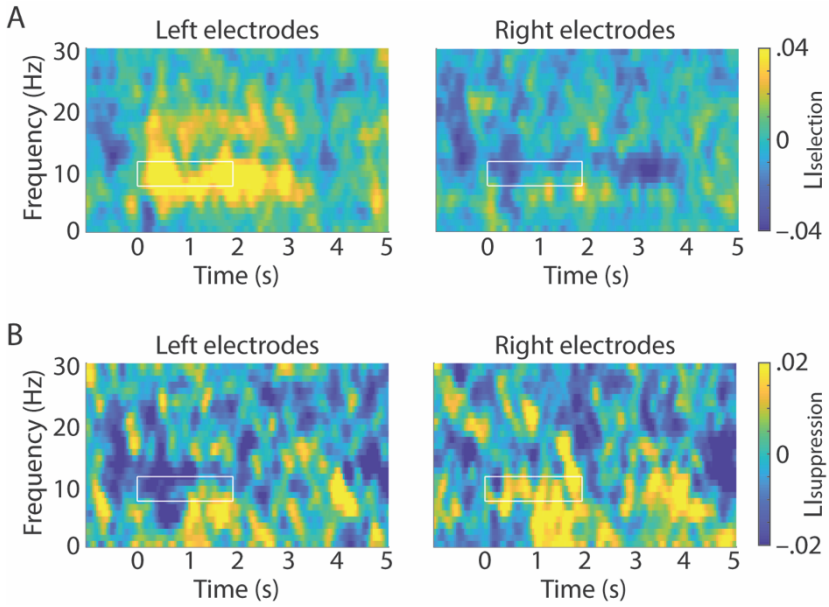

Figure S1. Time-frequency representations on the left and right show the respective grand-average lateralization index at 12 left- and 12 right-hemispheric electrodes (electrodes highlighted in Fig. 2 B&D). (**A**) Lateralization index for the selection of lateralized targets ($LI_{selection}$). (**B**) Lateralization index for the suppression of lateralized distractors ($LI_{suppression}$). White outlines indicate the time-frequency region of interest before the onset of tone sequences (0–1.9 s; 8–12 Hz).

Analysis of saccadic eye movements. Although participants were instructed to keep central gaze during the entire experiment, it might be that systematic differences in saccadic eye movements for our spatial selection/suppression conditions confounded the results. To rule this out, we inspected the EEG for independent components tuned to vertical saccadic eye movements.

Prior to the start of the actual experiment, each participant performed a brief eye movement task. This was done in order to obtain an objective measure of possible eye movements during the spatial task. Participants followed a dot on the screen that jumped eight times either horizontally (up and down by ~8° visual angle) or vertically (left and right by ~8° visual angle) with inter-jump-intervals of 1s. The task started with a vertical movement trial and then alternated between horizontal and vertical movement trials.

Trials of the eye movement task were segmented into epochs relative to the onset of the first jump of the dot (−1 to +10s). An independent component analysis (ICA) was used to extract one component for vertical eye movements for each participant (horizontal eye movements were not considered further in this study). The event-related potential (ERP) across all participant's vertical eye movement components clearly differentiated between saccades to the left versus right side (Fig. S2 A).

To control for potential confounds of vertical saccadic eye movements in the EEG data of the spatial attention task, we projected each participant's raw task data (with no trials rejected) through the vertical eye movement component, followed by computation of the event-related potential (ERP). For statistical analysis, we performed two cluster-based permutation tests to contrast the ERP during trials of the spatial attention task (0 to 4 s) for target selection on the left versus right side and distractor suppression on the left versus right side, respectively. In essence, these cluster-based permutation tests cluster *t*-values of adjacent bins in time-electrode space (minimum cluster size: 3 adjacent electrodes) and compare the summed *t*-statistic of the observed cluster against 10,000 randomly drawn clusters from the same data with permuted condition labels. The *p*-value of a cluster corresponds to the proportion of Monte Carlo iterations in which the summed *t*-statistic of the observed cluster is exceeded (two-sided testing; alpha level of 0.05).

ERPs of task data projected through the vertical eye movement component did not show differences between experimental conditions (Fig. S2 B). Cluster permutation tests revealed no significant differences in the ERP for selection of targets on the left versus right side (all cluster *p*-values > 0.19) or suppression of distractors on the left versus right side (all cluster *p*-values > 0.36).

These results suggest that participants complied with our task instructions and did not systematically perform saccadic eye-movements to or away from the to-be-selected or to-be-suppressed loudspeaker.

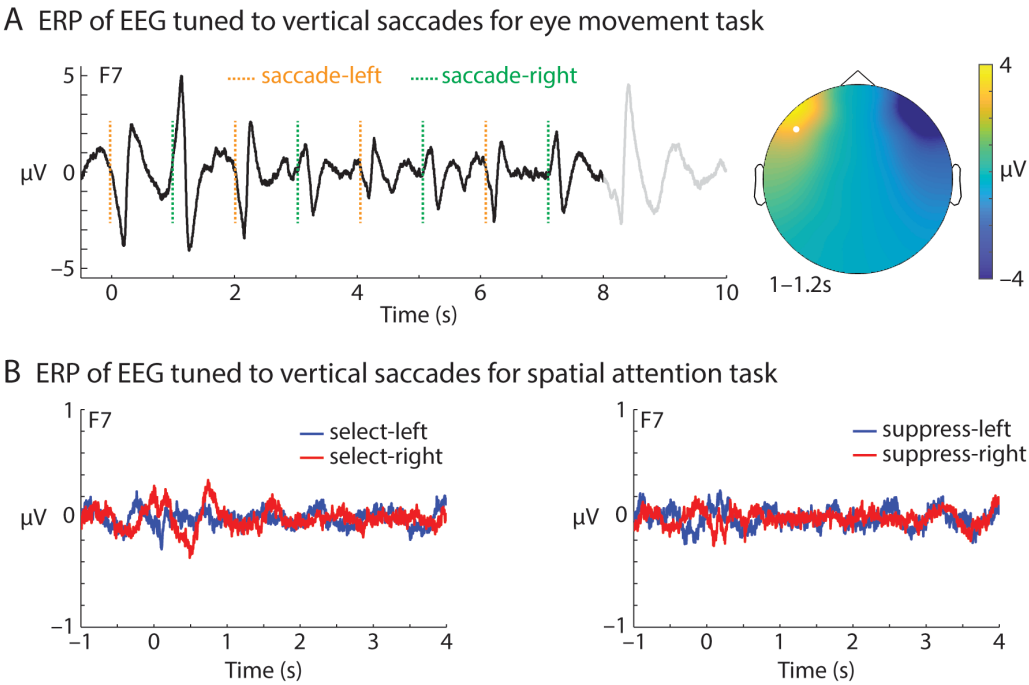

Figure S2. (**A**) During a pre-experiment eye-movement task participants followed a dot, which jumped eight times from the left to the right side on the screen, with their gaze. The grand-average event-related potential (ERP; at electrode F7) was computed on the EEG data projected through one vertical saccade component per participant (N = 33). At 8 s, participants performed an additional saccade back to the center of the screen to read task instructions. The topographic map shows ERP amplitude (1–1.2s) following the onset of one saccade to the right side (electrode F7 highlighted). (**B**) EEG data during the spatial attention task were projected through the same vertical saccade component for each participant as in (A). Grand-average ERPs for spatial attention (left panel) and spatial suppression (right panel) show no obvious saccade-related activity in trials with targets or distractors on the left versus right side.

Relation of $LI_{selection}$ and $LI_{suppression}$ on the source level. To further explore the non-significant correlation of $LI_{selection}$ and $LI_{suppression}$ found on the sensor level (Fig. 3A), we calculated the Spearman correlation coefficient for $LI_{selection}$ and $LI_{suppression}$ at each voxel in source space (Fig. S3). As explained in the manuscript, a negative correlation would be expected if these two neural signatures instantiate the same underlying cognitive faculty. To the contrary, the correlation on the source level was weakly positive in widespread regions of the left hemisphere, which agrees with the weak but non-significant positive correlation of $LI_{selection}$ and $LI_{suppression}$ on the sensor level (Fig. 3A).

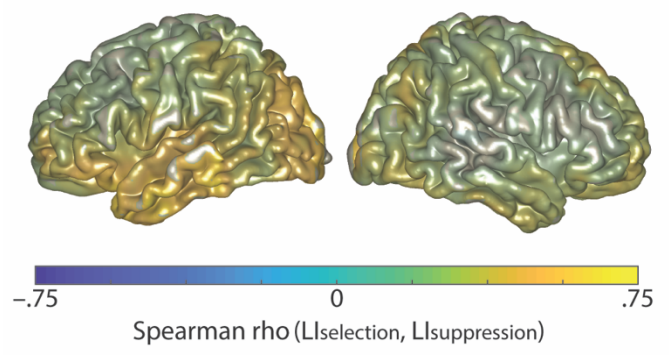

Figure S3. Colors on cortical surface indicate the Spearman rho correlation coefficient, which quantifies the relation of N = 33 participants' $LI_{selection}$ and $LI_{suppression}$ values on the source level.

Additional analyses of behavioral data. Tables S1–S3 below summarize results of three linear mixed-effects models to predict different single-trial behavioral outcome variables (Table S1: Confidence-weighted accuracy; Table S2: Raw accuracy; Table S3: Response time) on the predictors titrated pitch difference (within both tone sequences), congruency of pitch direction across target and distractor tone sequence (congruent versus incongruent), location of lateralized loudspeaker (left versus right), and role of lateralized loudspeaker (target versus distractor).

Table S1. Summary table of a linear mixed-effects model to predict the outcome variable confidence-weighted accuracy, using the model formula: Confidence-weighted accuracy ~ 1 + Titrated pitch difference + Congruency of pitch direction * Location of lateralized loudspeaker * Role of lateralized loudspeaker + (1|Participant ID). Degrees of freedom = 16949. Rows for predictors with p < 0.1 have gray shading.

Predictor	Estimate	t-statistic	p-value
Intercept	0.2932	6.618	<0.001
Titrated pitch difference	0.1558	10.031	<0.001
Congruency of pitch direction	0.175	8.572	<0.001
Location of lateralized loudspeaker	–0.0071	–0.3548	0.7228
Role of lateralized loudspeaker	–0.1151	–5.622	<0.001
Congruency * Location	–0.0264	–0.932	0.3513
Congruency * Role	0.0798	2.764	0.0057
Location * Role	0.051	1.803	0.0713
Congruency * Location * Role	0.0128	0.3203	0.7488

Table S2. Summary table of a generalized linear mixed-effects model (logit link function) to predict the outcome variable raw accuracy, using the model formula: Raw accuracy ~ 1 + Titrated pitch difference + Congruency of pitch direction * Location of lateralized loudspeaker * Role of lateralized loudspeaker + (1|Participant ID). Degrees of freedom = 17005. Rows for predictors with p < 0.1 have gray shading.

Predictor	Estimate	t-statistic	p-value
Intercept	0.7526	7.42	<0.001
Titrated pitch difference	0.3532	7.158	<0.001
Congruency of pitch direction	0.5166	7.221	<0.001
Location of lateralized loudspeaker	0.0305	0.4617	0.6443
Role of lateralized loudspeaker	–0.2576	–3.881	<0.001
Congruency * Location	–0.0248	–0.2493	0.8031
Congruency * Role	0.2958	2.94	0.0033
Location * Role	0.0225	0.2445	0.8069
Congruency * Location * Role	–0.0635	–0.4541	0.6497

Table S3. Summary table of a linear mixed-effects model to predict the outcome variable log-transformed response time, using the model formula: Log-transformed response time ~ 1 + Titrated pitch difference + Congruency of pitch direction * Location of lateralized loudspeaker * Role of lateralized loudspeaker + (1|Participant ID). Degrees of freedom = 17005. Rows for predictors with p < 0.1 have gray shading.

Predictor	Estimate	t-statistic	p-value
Intercept	–1.31	–6.319	<0.001
Titrated pitch difference	–0.2107	–3.822	<0.001
Congruency of pitch direction	–0.2291	–3.249	0.0012
Location of lateralized loudspeaker	0.1138	1.647	0.0996
Role of lateralized loudspeaker	0.1224	1.729	0.0838
Congruency * Location	0.0597	0.6103	0.5416
Congruency * Role	–0.0236	–0.2364	0.8131
Location * Role	-0.0372	–0.3807	0.7034
Congruency * Location * Role	–0.1829	–1.321	0.1864